объединенный
институт
ядерных
исследований
дубна

E13-93-308

ENERGY RESOLUTION OF A LEAD SCINTILLATING FIBER ELECTROMAGNETIC CALORIMETER

Submitted to «Nuclear Instruments and Methods»

1993

1 Introduction

The particle detectors which will be used at future accelerators (UNK, SSC, or LHC) must not only have good energy and space resolutions but also fast response and high radiation resistance. An intense search is currently underway to find calorimeter technologies which satisfy these stringent requirements. Lead-scintillating fiber electromagnetic calorimeters [1] — [7] are attractive candidates.

We built a lead scintillating fiber (SciFi) calorimeter module and tested it in electron and pion beams in the energy region from 5 to 70 GeV. In our experimental and Monte Carlo (MC) studies we concentrated on the energy resolution of the calorimeter module. The energy resolution of a SciFi calorimeter is influenced by many factors, among the most important are:

- the volume ratio R of passive (absorber) to active (fibers) material;
- the characteristics of the fibers: transparency, fiber radius, light output;
- the tilt angle (i.e. the angle between the particle direction and the axis of fiber in the horizontal plane);
- the level of light reflection at fiber end (reflectivity).

The basic experimental studies were carried out at a tilt angle of 3° with a module of the size $10 \times 10 \times 30\ cm^3$. In the MC studies the experimental conditions were carefully simulated with the particular emphasis on the influence of the light attenuation in fibers and the level of light reflection at fiber end on the energy resolution of the calorimeter module.

2 Simulation Results

The MC calculations were carried out for a block of the size 20 × 20 × 40 cm^3. A sub-block with the same dimensions as the experimental module was defined (called in the following the experimental block). Such a structure was chosen to study effects of the energy leakage on the experimental module energy resolution. All other parameters were taken to be the same as in the real module:

i) material volume ratios $(lead : glue : fiber)$: 1 : 0.17 : 1;

ii) fiber diameter: $d = 1\ mm$;

iii) tilt angle: $\theta = 3°$.

We analyzed the energy resolution using the resolution formula:

$$\frac{\sigma}{E} = \frac{a}{\sqrt{E}} \oplus b. \qquad (1)$$

The coefficient a represents the combined effect of sampling fluctuations (a_1) and photostatistics fluctuations (a_2), namely $a = \sqrt{a_1^2 + a_2^2}$. The coefficient b characterizes effects connected with energy leakage, tilt angle, light attenuation, reflectivity, etc.

The MC code is based on the GEANT3 package [8]. The passive material has been treated as a mixture of lead and epoxy glue. The kinetic energy cuts for both electrons and gammas have been taken down to 10 keV. To treat the light attenuation in fibers and the reflectivity, the energy deposited in the fibers has been multiplied by a weight factor:

$$W = exp\left(-\frac{l}{\lambda}\right) + r\, exp\left(-\frac{2L-l}{\lambda}\right), \qquad (2)$$

where l is the distance from the place of energy release to the place of light collection, L is the fiber length, λ is the attenuation length, and r is the reflectivity.

The results of simulation are summarized in the following tables and figures. In Table 1 and Fig. 1 are compared the energy resolution of full block with that of experimental block in the case when ideal conditions are assumed (no light attenuation i.e. $\lambda = \infty$). The resolution of the full block is slightly better than that of the experimental one, but the improvement is not statistically significant. We conclude that if the attenuation and photostatistics are ignored then the energy resolution of the experimental block should be:

$$\frac{\sigma}{E}\ (\%) = \frac{11.31 \pm 0.36}{\sqrt{E}} \oplus 0.53 \pm 0.27.$$

It is important to know how the energy resolution of a calorimeter is affected by such fiber parameters like the fiber attenuation length and reflectivity. We carried out a detailed MC analysis of this dependence. The energy resolution for the incident energies 5, 10, 15, 20 and 50 GeV at various conditions, characterized by the different attenuation lengths (50, 75, 150 and ∞ cm) and reflectivity (0%, 40%, 70% and 100%) were investigated. The energy resolution of calorimeter block for these different conditions is given in Table 2. From this table we see the strong dependence of b on attenuation, namely the constant term b increases with decreasing attenuation length λ. This dependence is weaker as the reflectivity r is increased. The coefficient a shows little dependence on attenuation or reflection, though a small tendency to increase with decreasing λ is noticeable especially at low values of r. The dependence of b on attenuation at fixed reflectivity and vice-versa is shown in Fig. 2a - 2b.

We conclude that the attenuation of light as well as the light reflection at fiber end have significant influence on energy resolution especially on constant term (b).

3 Fabrication of Scintillating Fiber Calorimeter

3.1 Selection of Scintillating Fibers

The scintillating fibers with a polymethylmethacrylate (PMMA) were prepared and produced in the Engineering Center of Polymer Optical Fibers (Tver, Russia). The cladding was made of fluoracrylat with fluor in different concentrations. The fiber surface was not blackened. We measured the light attenuation length for various types of fibers, which differred by luminofors, type of cladding, etc., with diameters in the range 0.9–1.1 mm. The diagram

of the apparatus used is shown in Fig. 3. The fibers have been excited in two ways: by a nitrogen laser and by ultraviolet xenon lamp (UV). In both cases the results are practically identical, so we refer only to the results obtained in the second way. The measurement was made both with a yellow light filter placed in front of the photomultiplier (PM) and without it. The detailed results on the light attenuation measurement in different types of fibers will be published in a separate paper.

The dependence of the mean amplitude on the place of the excitation is shown in Fig. 4 for a fiber length of 60 *cm*. The experimental points were approximated by the formula:

$$Y = A\ exp(-X/\lambda_1) + B\ exp(-X/\lambda_2) \qquad (3)$$

and the results of the approximation for various types of fibers are presented in Table 3.

As reported in the papers [10, 11], where the attenuation length was measured by means of a radiation source, there are two distinct attenuation lengths λ_1 and λ_2 for the fiber. In our case λ_1 is between 1.7 and 4.2 *cm* and λ_2 – between 57 and 98 *cm*.

One should notice that the formula (3) is only a simple approximation for light attenuation in the fiber. By fitting the measurements made on the fibers of the same type, but of different lengths, one will describe satisfactorily the measurements with (3) in each case. However, the fitted values of λ_1 and λ_2 were found not to be the same for measurements done on fibers of different lengths, as can be seen from Table 3 where the results of measurements made for fibers of 60 *cm* and 125 *cm* are given. This can be easily understood, because the process of the light propagation in the fibers is too complex to be described by a simple formula like (3); for example we didn't take into account the light reflection on one end of the fiber (see for example Eq. (2) where the fiber length appears explicitely and such a dependence is 'propagated' in the dependence of λ_1 and λ_2 on fiber length). Therefore, in this paper, the values for λ_1 and λ_2 should be interpreted as some kind of effective values rather than as intrinsic characteristics of the fiber. In order to have a correct estimation of light attenuation in a calorimeter block one should use the values of λ_1 and λ_2 obtained from measurements made on fibers of the same lengths as in that block. Using results of the fit with Eq. (3) from measurements made on fibers with different lengths than those in the calorimeter block can give misleading results.

3.2 Module Structure

The fabrication technology is based on gluing profiled lead sheets. Several machines have been built for rolling the lead sheets. In Fig. 5 is shown a transverse section of the calorimeter block. One can see the profiles of lead sheets, the fibers, and how they are glued together with epoxy. Fibers with 1 *mm* diameter were embedded into the channels of the lead plate (71 fibers for one plate) by a thin layer of epoxy compound.

The type of fibers used in our module is printed in bold type in Table 3. The volume ratio of absorber (including epoxy) to fiber is $R = 1.17 : 1$. The effective radiation length and interaction length are $X_0 = 1.05$ *cm* and $\Lambda_{int} = 31.05$ *cm* respectively.

The module dimensions are $10 \times 10 \times 30\ cm^3$. The total number of the fibers is 5600. The length of the fiber ends protruding from the lead plate is 20 *cm*. The fibers were bundled together and glued by epoxy, polished and connected through a tapered circular light guide (length ~ 5 *cm*) to a FEU-110 photomultiplier by means of optical grease. As the fibers are extended by 20 *cm* from the rear of the module, elimination of short attenuation length component is assured increasing the longitudinal uniformity of the calorimeter response.

A schematic diagram of the module is shown in Fig. 6.

4 Test Beam Results

The module was tested in the beam of positrons and π^+-mesons at 5 GeV in channel 18 of the Serpukhov accelerator U-70 and in the X5 electron test beam of the SPS CERN in the energy range 5–70 GeV. The tilt angle θ was about 3° in both cases. The response of the calorimeter to 5 GeV e^+ and hadrons (mainly π^+) is shown in Fig. 7 and 8 respectively. The π^+-spectrum is used for the assessment of photoconversion fluctuations (see below).

The calorimeter response (the mean value of the signal amplitude in ADC channels) as a function of energy is shown in Fig. 9. The behavior of this dependence is very close to a linear function over the large energy range.

In Fig. 10 the energy resolution is plotted versus the incident energy. The experimental values of the energy resolution can be approximated by:

$$\sigma/E = (13.13 \pm 0.29)/\sqrt{E} \oplus (1.74 \pm 0.09)$$

or

$$\sigma/E = (11.23 \pm 0.40)/\sqrt{E} + (0.96 \pm 0.08),$$

where the first expression assumes the two terms are added quadratically and the second assumes the two are added linearly. The result is in a good agreement with the simulation results, if photoconversion is taken into account (see below).

In Table 4 are presented the energy resolution of the SciFi calorimeters. A direct comparison between these results is difficult to do because their parameters (absorber/fiber ratio), or experimental conditions (tilt angle) are different. However, our results are consistent with those obtained with roughly similar experimental conditions.

In order to examine the behavior of the signal attenuation along the module length we exposed it to a 5 GeV e^+-beam perpendicular to the fibers at several distances from the PM. The mean value of the amplitude as a function of the position of the beam is shown in Fig. 11. The solid line is the result of the approximation by the formula:

$$Y = A\ exp(-X/\lambda)$$

where the parameter $\lambda = 81.8\ cm$. In these measurements the light reflection from the end of fiber was suppressed.

4.1 Comparison with Monte Carlo

To compare the experimental results with MC we have to take into account the following:

i) the reflectivity;

ii) the photostatistics fluctuations.

We estimate that due to the absence of a mirror at the end of the fiber, the reflectivity is not more than 30-40%. So we can use the simulation results for reflectivity 0% and 40% (Table 2) and interpolate between the values of the energy resolution at λ=75 *cm* and λ=150 *cm* to the attenuation length $\lambda = 81.8\ cm$ for both values of the reflectivity. As will be shown below (see Fig. 13), after the introduction of the effects of photostatistics, the experimental values of resolution lay in a corridor drawn by the MC resolution curves for $r = 0\%$ and $r = 40\%$ in the whole energy range.

Fluctuations due to photostatistics are governed by the average number of photoelectrons created per 1 GeV of incident energy (n_{phe}), and the coefficient a_2 characterizing these fluctuations (c. f. Eq. (1)) can be expressed by [12]:

$$a_2 = f_m/\sqrt{n_{phe}},$$

where $f_m = 1.17 \div 1.22$ is a factor characterizing the increase of photostatistics standard deviation due to multiplication of charge in PM dynode system while the factor $1/\sqrt{n_{phe}}$ is due to Poisson statistics.

To estimate a_2 we have compared the experimental and MC calorimeter response to pions (in the calorimeter block $10 \times 10 \times 30\ cm^3$, Fig. 12). In the MC simulation of the π^+ passage through the calorimeter block only electromagnetic processes were considered and fluctuations due to photostatistics were ignored. The experimental spectrum presents the real calorimeter response which also includes errors due to photostatistics. Moreover it includes also a "hadronic tail" corresponding to events with nuclear interaction of π^+. If the "hadronic tail" is removed from the experimental spectrum then the spectrum can be treated as a convolution of the MC spectrum and the PM response function. Hence deconvolution of the experimental spectrum will reveal the coefficient a_2. Practically, for the purpose of extracting a_2 we fitted the MC spectrum by a linear combination of two Gaussians and the experimental one by a linear combination of a Gaussian and a gamma function. The second Gaussian in the MC case was used for removing the "Landau tail" from the spectrum. On the other hand the gamma function was used for removing both the "hadronic" and the "Landau" tails from the experimental spectrum. The Gaussian part of the experimental spectrum is wider, compared to the corresponding MC one, due to photostatistics fluctuations. Finding the parameters of the Gaussian distributions (i.e. mean value and standard deviation) in both the experimental (A^{ex}, σ^{ex}) and MC spectra (

A^{MC}, σ^{MC}) allows to define the fluctuations connected with photostatistics:

$$\frac{a_2}{\sqrt{E^{\pi}_{abs}}} = \sqrt{\left(\frac{\sigma^{ex}}{A^{ex}}\right)^2 - \left(\frac{\sigma^{MC}}{A^{MC}}\right)^2}, \qquad (4)$$

where E^{π}_{abs} is the average energy loss of 5 GeV π^+ in the calorimeter block. From the simulation, we obtained $E^{\pi}_{abs} = 0.31$ GeV and from the fitting procedure $\sigma^{ex}/A^{ex} = (17.02 \pm 1.14)$ % and $\sigma^{MC}/A^{MC} = (13.12 \pm 0.31)$ %. We obtained:

$$a_2 = (6.04 \pm 1.02)\ \%,$$

which corresponds to approximatelly 400 photoelectrons per 1 GeV. We note that the value of the coefficient should be treated as an crude estimate rather than an exact value.

Now we can correct the MC spectra for effect due to photostatistics (see Eq. (1) and below). In Fig. 13 are compared the corrected MC resolutions (dashed lines) for $\lambda = 81.8$ *cm* at two values of reflectivity ($r = 0$ and $r = 40\%$) with the experimental points. We see that the experimental results are in very good agreement with MC ones.

5 Conclusions

The energy resolution of a SciFi calorimeter module made on the basis of scintillating fibers with diameter 1 *mm* and attenuation length about 80 *cm* (the lead-to-fiber volume ratio 1.17 : 1) may be expressed by the formula:

$$\sigma/E(\%) = 13.1/\sqrt{E} \oplus 1.7$$

The results are in good agreement with the simulation and correspond to the results obtained by the similar calorimeters elsewhere.

A Monte Carlo analysis of the dependence of energy resolution on light attenuation length (λ) and light reflection at front edge of calorimeter (r) was carried out. The significant dependence of constant term (b) on λ and r was observed.

Table 1

Monte Carlo Energy Resolution for Calorimeter blocks $20 \times 20 \times 40$ cm^3 and $10 \times 10 \times 30$ cm^3 respectively

	block $20 \times 20 \times 40$ cm^3	block $10 \times 10 \times 30$ cm^3
E_{inc} (GeV)	Energy resolution (%) $\pm$ its Error (%)	
5	4.95 $\pm$ 0.18	5.07 $\pm$ 0.18
10	3.47 $\pm$ 0.13	3.56 $\pm$ 0.14
15	3.02 $\pm$ 0.14	3.05 $\pm$ 0.14
20	2.56 $\pm$ 0.12	2.60 $\pm$ 0.12
50	1.61 $\pm$ 0.11	1.66 $\pm$ 0.11
Resolution	$\frac{11.09 \pm 0.32}{\sqrt{E}} \oplus 0.50 \pm 0.27$	$\frac{11.31 \pm 0.36}{\sqrt{E}} \oplus 0.53 \pm 0.27$

Table 2

Resolution Parameters (a, b) vs. Reflection (r), Attenuation (λ)

r	λ (cm)	$a \pm \Delta a$ (%)	$b \pm \Delta b$ (%)
Simulation Block ($20 \times 20 \times 40$ cm^3)			
1.00	∞	11.09 $\pm$ 0.32	0.50 $\pm$ 0.27
Experimental Block ($10 \times 10 \times 30$ cm^3)			
0.00	∞	11.31 $\pm$ 0.36	0.53 $\pm$ 0.27
0.00	150.00	11.59 $\pm$ 0.41	1.21 $\pm$ 0.24
0.00	75.00	11.80 $\pm$ 0.53	2.17 $\pm$ 0.22
0.00	50.00	11.99 $\pm$ 0.67	3.17 $\pm$ 0.22
0.40	∞	11.31 $\pm$ 0.36	0.53 $\pm$ 0.27
0.40	150.00	11.45 $\pm$ 0.35	0.78 $\pm$ 0.31
0.40	75.00	11.57 $\pm$ 0.42	1.31 $\pm$ 0.24
0.40	50.00	11.64 $\pm$ 0.51	2.01 $\pm$ 0.21
0.70	∞	11.31 $\pm$ 0.36	0.53 $\pm$ 0.27
0.70	150.00	11.38 $\pm$ 0.31	0.62 $\pm$ 0.35
0.70	75.00	11.46 $\pm$ 0.37	0.92 $\pm$ 0.27
0.70	50.00	11.51 $\pm$ 0.43	1.43 $\pm$ 0.23
1.00	∞	11.31 $\pm$ 0.36	0.53 $\pm$ 0.27
1.00	150.00	11.33 $\pm$ 0.36	0.54 $\pm$ 0.27
1.00	75.00	11.38 $\pm$ 0.36	0.67 $\pm$ 0.33
1.00	50.00	11.41 $\pm$ 0.39	0.99 $\pm$ 0.27

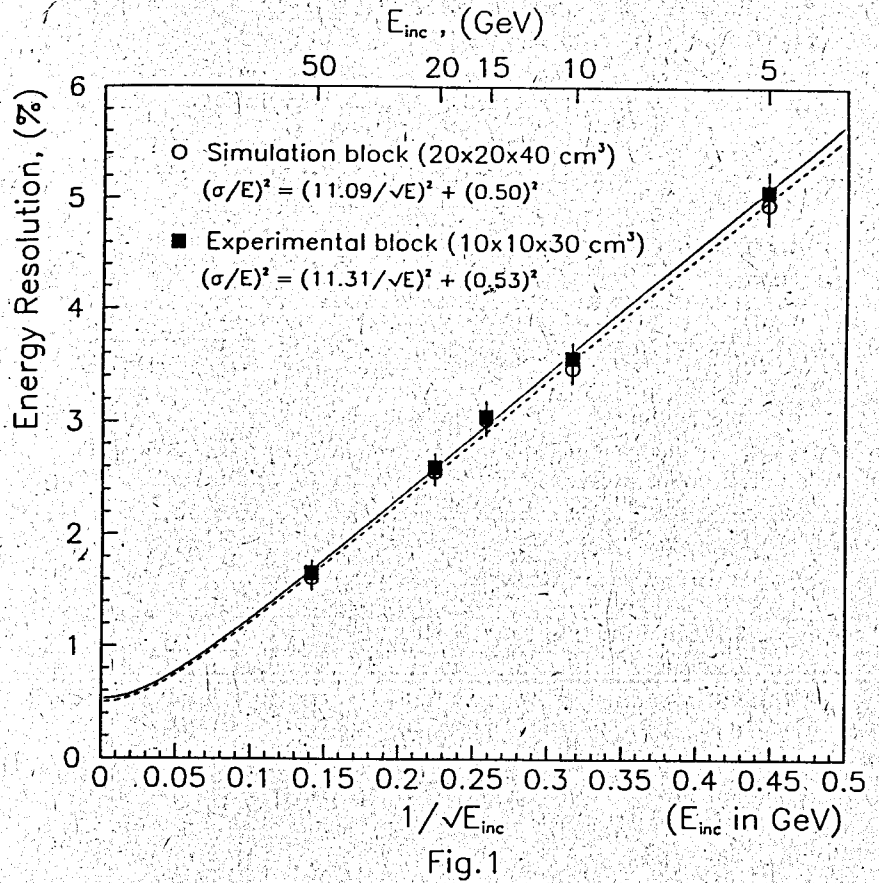

Fig.1

Fig. 1: Monte Carlo results on energy resolution vs. incident energy in the ideal case (attenuation length $\lambda = \infty$ and reflectivity $r = 100\ \%$) for two block sizes:

i) $(11.09 \pm 0.32)/\sqrt{E} \oplus 0.50 \pm 0.27$ (block $20 \times 20 \times 40\ cm^3$);

ii) $(11.31 \pm 0.36)/\sqrt{E} \oplus 0.53 \pm 0.27$ (block $10 \times 10 \times 30\ cm^3$).

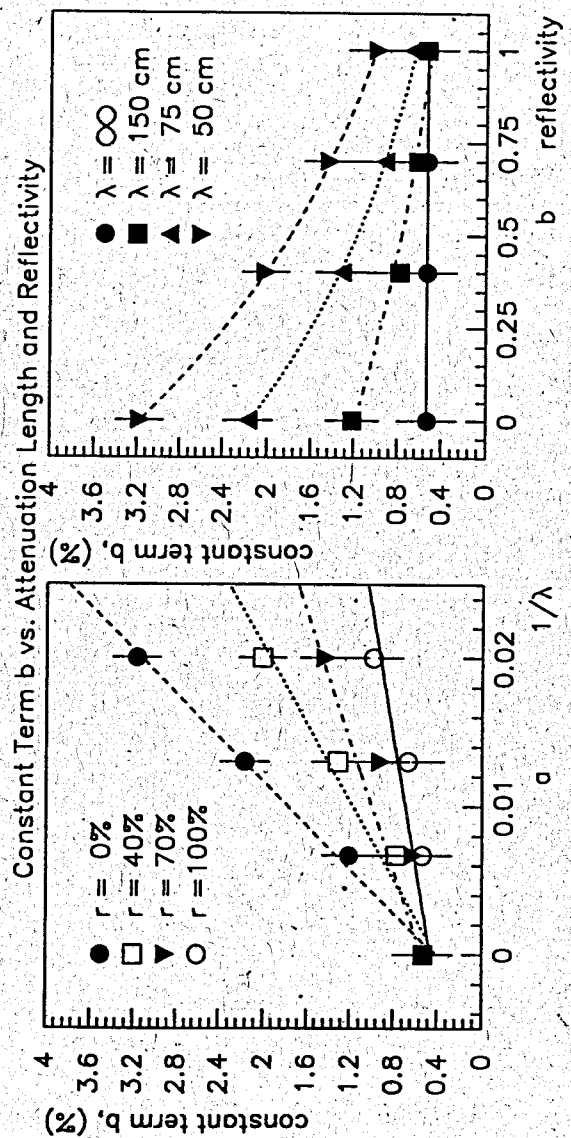

Fig. 2: The energy resolution: the constant term b vs. attenuation length (λ) and reflectivity (r):
a) b vs. λ at different r;
b) b vs. r at different λ.

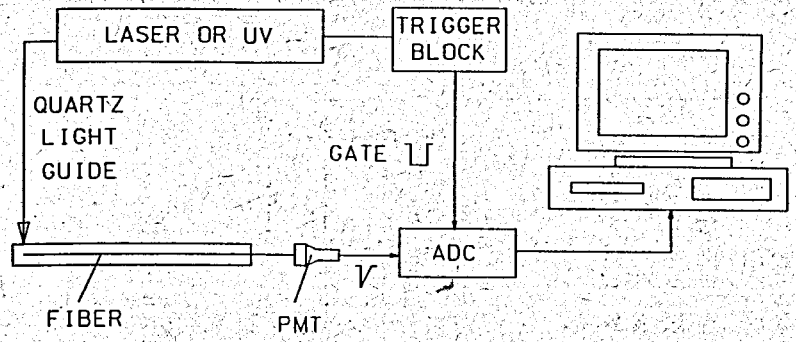

Fig. 3: Diagram of the experimental setup for measurement of attenuation length.

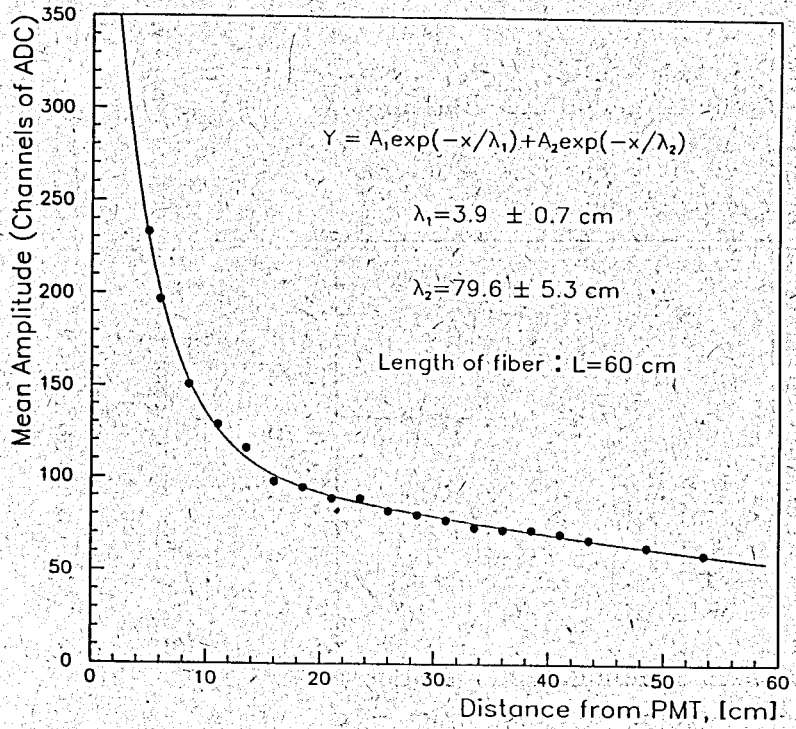

Fig. 4: Dependence of mean amplitude on the distance from the place of excitation (for fibers of 60 *cm* length).

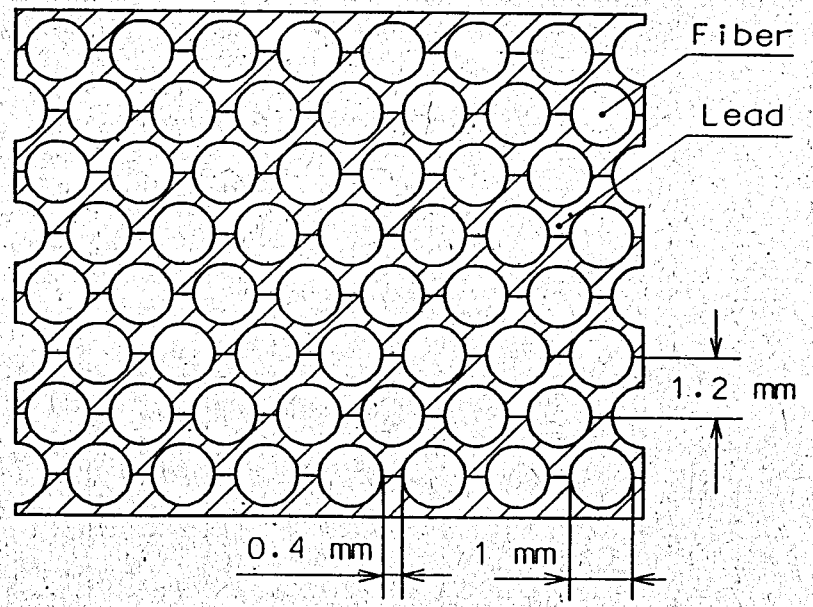

Fig. 5: Transverse section in the calorimeter block.

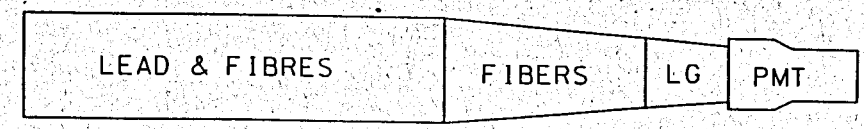

Fig. 6: Schematic diagram of the experimental module.

Table 3
Attenuation Length for Some Fibers; Influence of Fiber Length

No.	Fiber Type	Fiber Length L = 120 *cm*		L = 60 *cm*	
		λ_1 (*cm*)	λ_2 (*cm*)	λ_1 (*cm*)	λ_2 (*cm*)
1	H-111	5.4	124	3.6	98
2	H-122	5.4	124	3.6	98
3	**H-130**	**9.0**	**122**	**3.9**	**87**
4	H-137	4.9	115	2.4	91
5	H-140	5.5	121	3.4	83
6	H-142	5.2	142	4.2	84
7	H-143	7.9	121	3.3	65
8	H-144	9.7	119	3.2	67
9	H-145	8.9	132	2.9	57
10	H-141	5.7	122	4.0	81
11	H-136	11.7	142	1.7	83

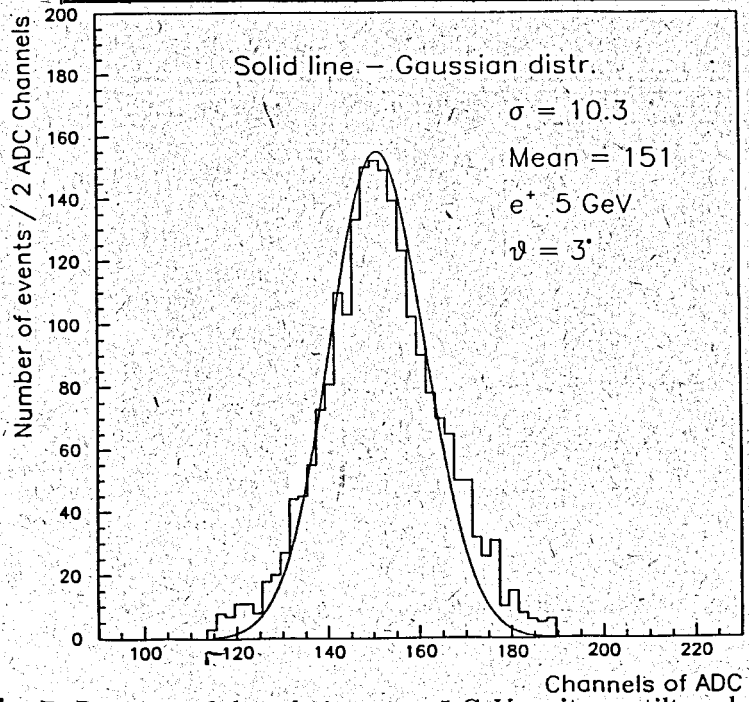

Fig. 7: Response of the calorimeter to 5 GeV positrons; tilt angle $\theta = 3°$.

Table 4
The Energy Resolution of Lead/Scintillating Fiber Calorimeters

No.	Energy [GeV]	Angle [deg.]	Eff. Radiation Length [*cm*]	Resolution σ/E [%]	Refer.
1	0.04–1	90	1.1	$9.8/\sqrt{E}$	[1]
2	0.5–50	≤ 0.6	1.1	$10/\sqrt{E}+2.2$	[2]
3	1–3.5	1.7–17	0.85	$20/\sqrt{E}$	[3]
4	10–50	0.5–13	1.3	$12/\sqrt{E}$	[4]
5	10–150	3	0.75	$13/\sqrt{E}+1.2$ $15.7/\sqrt{E}\oplus 2.$	[5] [5]
6	0.035–5	1.8–10	1.61	$6/\sqrt{E}$	[6]
7	9–37	≥ 3	0.45	$17/\sqrt{E}+2$	[7]
8	5–70	3	1.05	$11.2/\sqrt{E}+1.0$ $13.1/\sqrt{E}\oplus 1.7$	This paper

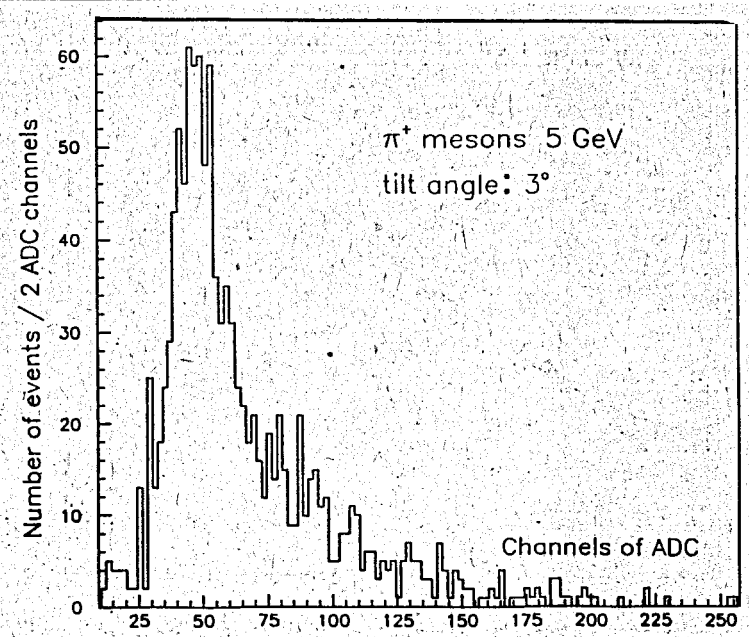

Fig. 8: Response of the calorimeter to 5 GeV π^+; tilt angle $\theta = 3°$.

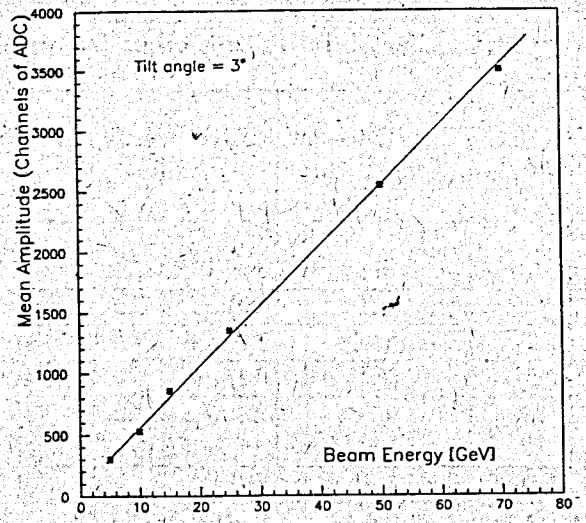

Fig. 9: Mean value of the calorimeter response (in ADC channels) vs. incident energy.

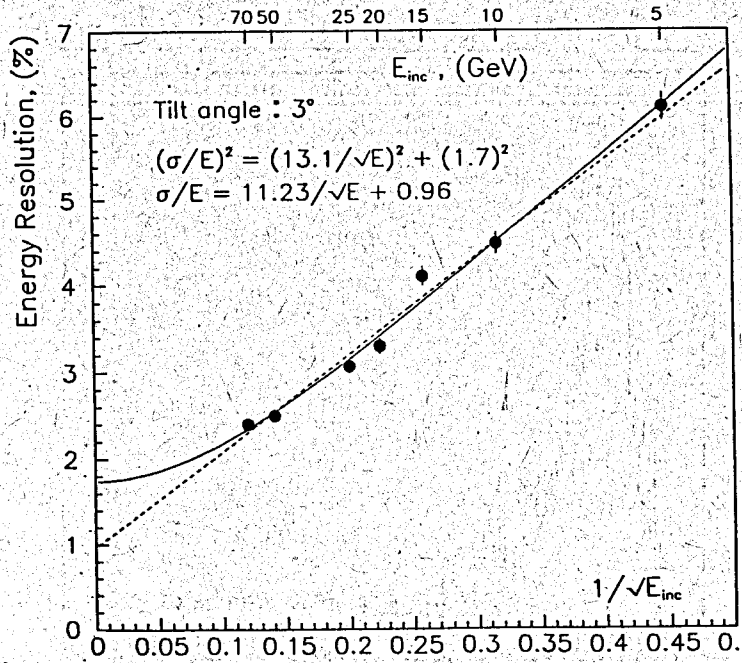

Fig. 10: Experimental energy resolution vs. incident energy; incident beam e^+; tilt angle 3°.

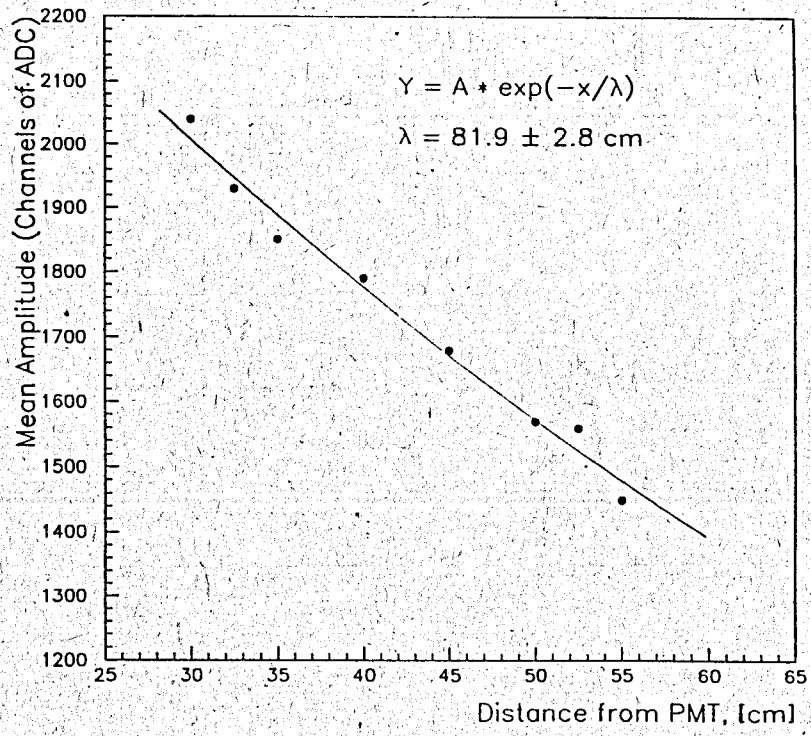

Fig. 11: The average amplitude for a 5 GeV e^+ beam, perpendicular to the fibers vs. distance from PM. The obtained attenuation length is 81.8 ± 2.8 cm.

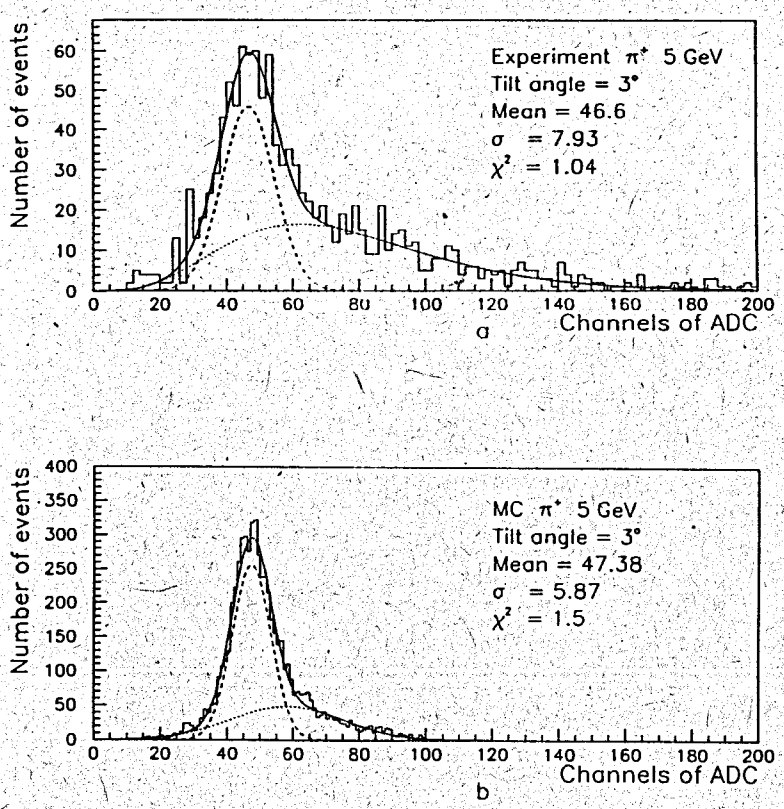

Fig. 12: The energy loss spectra for 5 GeV π^+:
a) experiment;
b) MC simulation.
In both cases, with dashed line are drawn separately the components of the fit function.

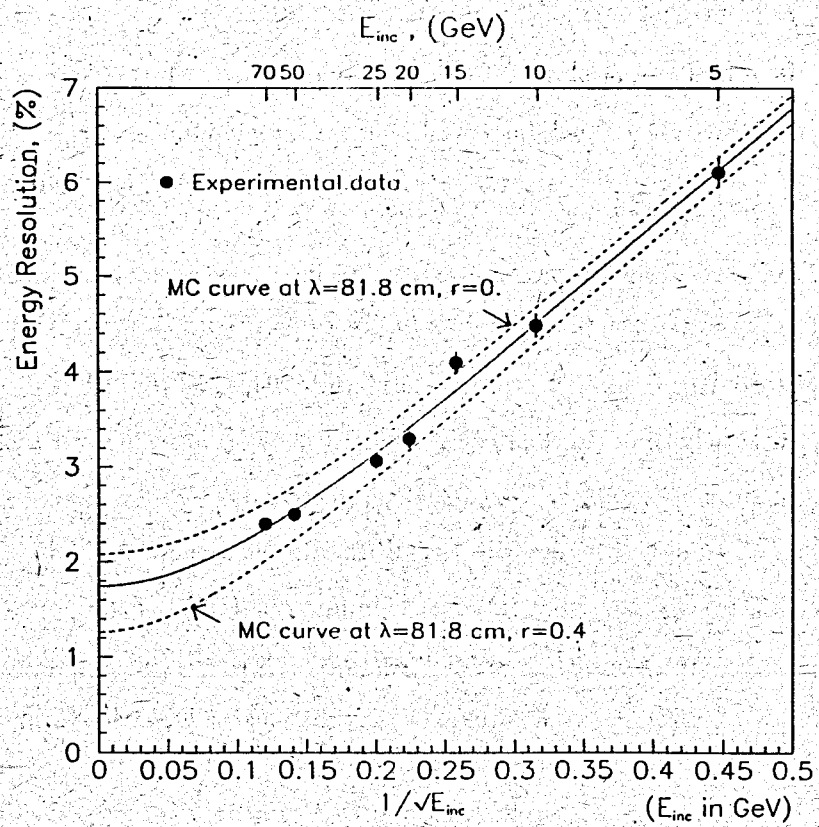

Fig. 13: Comparison of the experimental energy resolution with MC ones (at reflectivity 0 % and 40 %) corrected on photoconversion.

6 Acknowledgements

We would like to thank B. Kut'in, A. Blick, B. French and A. Kirk for their interest and support during the measurements at Serpukhov and CERN.

References

[1] H. Burmeister et al. Nucl. Instr. and Meth. A225, (1984), 530.

[2] P. Sonderegger, Nucl. Instr. and Meth. A257, (1987), 523.

[3] A. Baldit et al., NA38 proposal. CERN/SPSC/85-20 and CERN/SPSC/85-42.

[4] DELPHI Technical proposal, CERN/LEPS/83-3, (1983), p.148.

[5] D. Acosta et al., 1990, preprint CERN-EP/90-37, Geneva: CERN.

[6] D. Hertzog et al., Nucl. Instr. and Meth. A294, (1990), 446.

[7] R. Dzhelyadin et al.,1990, preprint IHEP 90-134, Serpukhov: IHEP.

[8] R. Brun et al., GEANT-CERN Program Library W5013.

[9] R. Wigmans, 1991, preprint CERN-PPE/91-39, Geneva: CERN.

[10] C. Hawkes et al., Nucl. Instr. and Meth. A292, (1990), 329.

[11] N. Amos et al., Nucl. Instr. and Meth. A297, (1990), 396.

[12] E. Funfer, H. Neuert, Zahlrohre un Szintillationszahler, Verlag G. Braun, Karlsruhe, 1959.

Received by Publishing Department
on August 9, 1993.